

Published in final edited form as:

*Chem Commun (Camb)*. 2013 November 4; 49(85): . doi:10.1039/c3cc45752d.

## Design of Oligothiophene-Based Tetrazoles for Laser-Triggered Photoclick Chemistry in Living Cells

Peng An<sup>a</sup>, Zhipeng Yu<sup>a</sup>, and Qing Lin<sup>a</sup>

Qing Lin: qinglin@buffalo.edu

<sup>a</sup>Department of Chemistry, State University of New York at Buffalo, Buffalo, NY 14260 (USA)

### Abstract

A 405 nm light-activatable terthiophene-based tetrazole was designed that reacts with a fumarate dipolarophile with the second-order rate constant  $k_2$  exceeding  $10^3 \text{ M}^{-1} \text{ s}^{-1}$ . The utility of this laser-activatable tetrazole in imaging microtubules in a spatiotemporally controlled manner in live cells was demonstrated.

Because of their inherent capacity of spatiotemporal control, light-triggered chemical reactions have been increasingly employed in the design of “smart” materials,<sup>1</sup> molecular motors,<sup>2</sup> and biological switches for controlling cell signaling.<sup>3</sup> While several light-induced “click”-type reactions<sup>4</sup> have been reported recently, invariably, these reactions are triggered by UV light with the wavelengths in the range of 300–365 nm, which limits their utility in biological systems because of the phototoxicity.<sup>5</sup>

We reported a photoinduced tetrazole-alkene cycloaddition reaction (“photoclick chemistry”)<sup>6</sup> recently and demonstrated that this bioorthogonal ligation reaction can be employed to label proteins in live mammalian cells.<sup>7</sup> A key step of this reaction involves UV light-induced rupture of the tetrazole ring to generate *in situ* a highly reactive nitrile imine dipole.<sup>8</sup> In our earlier efforts to minimize photodamage to cells, we extended the photoactivation wavelength from 302 nm to 365 nm by placing suitable aryl substituents on the tetrazole ring;<sup>9</sup> however, significant cellular stress could still result from 365 nm photoirradiation.<sup>10</sup> Furthermore, typical fluorescent microscopes are not equipped with 365 nm UV lasers, preventing a wider use of photoclick chemistry in biological studies. To overcome these limitations, herein we report the design and synthesis of oligothiophene-based, 405 nm laser-activatable tetrazoles, the characterization of their reaction kinetics with electron-deficient dipolarophiles, and their utility in spatiotemporally controlled imaging of microtubules in live mammalian cells.

In search for laser-activatable tetrazoles, we were attracted to oligothiophenes because: (i) linear  $\alpha,\alpha$ -linked oligothiophenes are electron-rich  $\pi$ -conjugated systems that exhibit large molar absorptivity and tunable absorption wavelengths depending on chain length;<sup>11</sup> (ii) structural similarity between tetrazole and thiophene rings allows insertion of the tetrazole ring into the oligothiophene chain without disrupting the planar conjugation system, and as a result minimizes light energy being consumed through  $\sigma$ -bond rotation;<sup>12</sup> and (iii) the thiophene ring can be readily functionalized for improved water-solubility and cell

Correspondence to: Qing Lin, qinglin@buffalo.edu.

†Electronic Supplementary Information (ESI) available: [details of any supplementary information available should be included here]. See DOI: 10.1039/b000000x/

‡Footnotes should appear here. These might include comments relevant to but not central to the matter under discussion, limited experimental and spectral data, and crystallographic data.

permeability.<sup>13</sup> Thus, a panel of oligothiophene-tetrazoles (**1–5**) were prepared by inserting the tetrazole ring into the bi-, ter-, and quater-thiophene structures (Scheme 1). A convergent synthetic route<sup>14</sup> was employed in which the substituted 5-(thiophen-2-yl)tetrazoles were coupled with the various phenyl(thiophen-2-yl)iodonium salts in the presence of Cu(OAc)<sub>2</sub> and NEt<sub>3</sub> (Schemes 1 and S1–S3).

To gain insights into the structural effect of embedding tetrazole into oligothiophenes, single crystals of oligothiophene-tetrazoles **2** and **4** were obtained and their structures were elucidated by X-ray crystallography (Fig. 1 and ESI). Both molecules adopt planar all-*trans* conformations and herringbone packing common to the known oligothiophenes.<sup>15</sup> The torsional angles between tetrazole and *N*-thiophene and between tetrazole and *C*-thiophene in compound **2** are 1.1° and 1.4° respectively, while the same torsional angles are less than 1° in compound **4** (evident from side views of Fig. 1a and 1b). The oligothiophene-tetrazoles are packed in the crystals through face-to-face  $\pi$ - $\pi$  interactions with  $\pi$ -distance of 3.4–3.4 Å. The electron-deficient tetrazole rings pack tightly against the electron-rich distal thiophene rings (Fig. 1b). Overall, the structure of terthiophene-tetrazole **2** closely matches that of quarter-thiophene<sup>15</sup>(Fig. 1c).

Since  $\pi$ -conjugation is retained in oligothiophene-tetrazoles, we measured UV-Vis absorption of the five tetrazoles in a mixed CH<sub>3</sub>CN/PBS (2:1) solvent (Fig. S1). As expected, the absorption maxima ( $\lambda_{\text{max}}$ ) showed significant bathochromic shift as the number of thiophene unit increases (Table 1); for tetrazoles with same number of thiophenes, the more thiophenes on the *N*-aryl side of the tetrazole, the greater the  $\lambda_{\text{max}}$  values (compare **2** to **3**; **4** to **5**). The order of  $\lambda_{\text{max}}$  is largely in agreement with the calculated HOMO-LUMO gaps with the exception of tetrazole **3** (Table 1). To our satisfaction, tetrazoles **2**, **4**, and **5** showed substantial absorption at 405 nm, a prerequisite for potential photoreactivity under 405 nm violet photoillumination.

To assess 405-nm photoactivatability, we subjected tetrazoles **1–5** with *mono*-methyl fumarate amide (MFA) under illumination of a diode laser (405 nm, 24 mW).<sup>16</sup> We chose MFA because it is an excellent dipolarophile for photoclick chemistry and is stable toward biological nucleophiles such as glutathione (Fig. S2). Among the oligothiophene-tetrazoles, tetrazole **2** showed the cleanest formation of the pyrazoline cycloadduct after 30 s photoillumination based on the HPLC traces (Fig. S3). A closer inspection of the pyrazoline cycloadducts by <sup>1</sup>H NMR revealed the formation of a pair of regioisomers in roughly 1:1 ratio with similar absorbance and fluorescence properties (Fig. S4). Importantly, quantum yield for 405 nm laser-induced tetrazole ring rupture was determined to be 0.16 based on chemical actinometer (Fig. S5), significantly higher than the 365 nm-photoactivatable tetrazoles we reported previously ( $\Phi = 0.006$ – $0.04$ ).<sup>9a</sup> While tetrazole **4** absorbs strongly at 405 nm, it gave rise to only trace amount of the pyrazoline cycloadducts (Fig. S6). Furthermore, despite its strongest absorbance, tetrazole **5** was found to be stable upon 405 nm photoillumination, likely due to its intrinsic fluorescence (Fig. S7).

To apply terthiophene-tetrazole **2** to cellular systems, a more water-soluble derivative **6** (Fig. 2a) was prepared by appending a negatively charged succinate at the distal thiophene ring (Scheme S5). To determine the reactivity of terthiophene-tetrazoles **2** and **6**, we performed the kinetic studies of the cycloaddition reactions with MFA under 405 nm photoirradiation. We found that the cycloaddition reactions proceeded very rapidly with the second-order rate constants ( $k_2$ ) determined to be  $619 \pm 108 \text{ M}^{-1} \text{ s}^{-1}$  and  $1299 \pm 110 \text{ M}^{-1} \text{ s}^{-1}$  for tetrazole **2** and **6**<sup>17</sup>, respectively (Fig. 2b, S8, S9), indicating a roughly twofold enhancement in reactivity for tetrazole **6**.

To probe whether tetrazole **6** allows laser-triggered photoclick chemistry *in vivo* in a spatiotemporally controlled manner, we tested the ability of tetrazole **6** to label microtubules<sup>18</sup> that are pre-treated with a fumarate-modified docetaxel in CHO cells. To this end, we synthesized a fumarate-docetaxel conjugate, IPFA-docetaxel, by attaching *mono*-isopropyl fumarate amide at position 10 of docetaxel *via* a flexible linker (Fig. 3a).<sup>19</sup> We used IFA-docetaxel because: (i) *mono*-isopropyl fumarate amide (IPFA) is more stable than mono-methyl fumarate amide *in vivo*;<sup>20</sup> (ii) modification at position 10 of docetaxel does not affect the binding of docetaxel to microtubules;<sup>21</sup> and (iii) IPFA exhibited similar reactivity as MFA in the cycloaddition reaction with tetrazole **2** (Fig. S11). Thus, we treated CHO cells with 40  $\mu$ M tetrazole **6** overnight and afterwards washed away the excess reagent with PBS. The cells were then incubated in OPTI-MEM medium containing 30  $\mu$ M IPFA-docetaxel for 30 min. A quadrangle area in the culture plate (Fig. 3b) was selected for intermittent photoirradiation with a 405 nm laser before fluorescence acquisition. In the fluorescence channel (ex = 458 nm, em = 531–623 nm), the quadrangle area showed a time-dependent turn-on fluorescence (Fig. 3b, top row), with average fluorescence intensity inside the illuminated quadrangle area roughly four-fold greater than outside after 48-sec exposure (Fig. S12). As a control, the same procedure without IPFA-docetaxel treatment led to only slight increase in background fluorescence inside the illuminated quadrangle area (Fig. 3b, bottom row), which can be attributed to the photogenerated, weakly fluorescent nitrile imine intermediates.<sup>7a</sup> To verify that the fluorescence is derived from microtubule-bound pyrazoline, in-cell fluorescence spectrum-scan was performed, revealing a maximum cytosolic emission at 548 nm (Fig. S13). Separately, we also measured the fluorescence spectrum of the preformed pyrazoline and found that it shows solvent-dependent fluorescence: it is non-fluorescent in PBS/acetonitrile (4:1), but strongly fluorescent in organic solvents along with a hypsochromic shift in emission maxima from 585 nm to 560 nm (Fig. S14). The blue-shifted in-cell fluorescence matches closely to that observed in organic solvents, suggesting that the generally formed pyrazoline-docetaxel likely binds to the microtubule surface with a low dielectric constant.

In summary, we have synthesized a panel of oligothiophene-based tetrazoles and found that a terthiophene-tetrazole gave excellent photoreactivity under 405 nm laser irradiation with ring rupture quantum yield of 0.16. A water-soluble terthiophene-tetrazole was then prepared that showed a faster reaction kinetics with a fumarate dipolarophile ( $k_2 = 1299 \pm 110 \text{ M}^{-1} \text{ s}^{-1}$ ) and capability for real-time spatiotemporally controlled imaging of microtubules *via* laser-triggered photoclick chemistry in live mammalian cells. Given that 405 nm laser is widely available on fluorescent microscope for exciting common fluorophores, we expect that this class of 405 nm laser-activatable thiophene-tetrazoles should facilitate a wider adoption of photoclick chemistry in cell biological studies.

## Supplementary Material

Refer to Web version on PubMed Central for supplementary material.

## Acknowledgments

This research was financially supported by the National Institutes of Health (GM 085092). We thank William Brennessel at the University of Rochester for solving X-ray structures of tetrazoles **2** and **4** (Cambridge Structural Database accession no. CCDC 931877 and 931876), and Alan Siegel at SUNY Buffalo Biological Sciences Imaging Facility (supported by the National Science Foundation Major Research Instrumentation grant DBI-0923133) for assistance with microscopy. P.A. is a visiting graduate student from Lanzhou University sponsored by China Scholarship Council.

## Notes and references

1. a) Kawata S, Kawata Y. *Chem Rev.* 2000; 100:1777. [PubMed: 11777420] b) Delaire J, Nakatani K. *Chem Rev.* 2000; 100:1817. [PubMed: 11777422]
2. a) Ruangsupipachat N, Pollard M, Harutyunran S, Feringa B. *Nat Chem.* 2011; 3:53. [PubMed: 21160518] b) Wang J, Feringa B. *Science.* 2011; 331:1429. [PubMed: 21310964]
3. Gorostiza P, Isacoff EY. *Science.* 2008; 322:395. [PubMed: 18927384]
4. Tasdelen MA, Yagci Y. *Angew Chem Int Ed.* 2013; 52:23. and references therein.
5. Sesto A, Navarro M, Burslem F, Jorcano JL. *Proc Natl Acad Sci USA.* 2002; 99:2965. [PubMed: 11867738]
6. a) Song W, Wang Y, Qu J, Madden MM, Lin Q. *Angew Chem Int Ed.* 2008; 47:2832. b) Song W, Wang Y, Qu J, Lin Q. *J Am Chem Soc.* 2008; 130:9654. [PubMed: 18593155] c) Lim RK, Lin Q. *Acc Chem Res.* 2011; 44:828. [PubMed: 21609129]
7. a) Song W, Wang Y, Yu Z, Vera CI, Qu J, Lin Q. *ACS Chem Biol.* 2010; 5:875. [PubMed: 20666508] b) Yu Z, Pan Y, Wang Z, Wang J, Lin Q. *Angew Chem Int Ed.* 2012; 51:10600.
8. a) Zheng SL, Wang Y, Yu Z, Lin Q, Coppens P. *J Am Chem Soc.* 2009; 131:18036. [PubMed: 19928921] b) Bégué D, Qiao GG, Wentrup C. *J Am Chem Soc.* 2012; 134:5339. [PubMed: 22364289]
9. a) Wang Y, Hu W, Song W, Lim RKV, Lin Q. *Org Lett.* 2008; 10:3725. [PubMed: 18671406] b) Yu Z, Ho LY, Wang Z, Lin Q. *Bioorg Med Chem Lett.* 2011; 21:5033. [PubMed: 21570845] c) Yu Z, Ho LY, Lin Q. *J Am Chem Soc.* 2011; 133:11912. [PubMed: 21736329]
10. Halliday GM, Byrne SN, Damian DL. *Semin Cutan Med Surg.* 2011; 30:214. [PubMed: 22123419]
11. a) Becker RS, Melo JS, Macanita AL, Elisei F. *J Phys Chem.* 1996; 100:18683. b) Adronov A, Malenfant PRL, Fréchet JM. *J Chem Mater.* 2000; 12:1463.
12. a) Gierschner J, Cornil J, Egelhaaf H-J. *Adv Mater.* 2007; 19:173. b) Fichou D. *J Chem Mater.* 2000; 10:571.
13. Mishra A, Ma C-Q, Bäuerle P. *Chem Rev.* 2009; 109:1141. [PubMed: 19209939]
14. Garfunkel J, Ezzili C, Rayl TJ, Hochstatter DJ, Hwang I, Boger DL. *J Med Chem.* 2008; 51:4392. [PubMed: 18630870]
15. a) Antolini L, Horowitz G, Kouki F, Garnier F. *Adv Mater.* 1998; 10:382. b) Siegrist T, Kloc C, Laudise RA, Katz HE, Haddon RC. *Adv Mater.* 1998; 10:379. c) Azumi R, Goto M, Honda K, Matsumoto M. *Bull Chem Soc Jpn.* 2003; 76:1561.
16. Light intensity value was recorded by placing a FieldMaster GS energy analyzer equipped with LM-10 HTD power meter sensor in the light path of the laser beam.
17. The quantum yield for ring rupture of tetrazole 6 was determined to be 0.15; see Fig. S5 in ESI for details.
18. a) Nicolaou KC, Dai WM, Guy RK. *Angew Chem, Int Ed.* 1994; 33:15. b) Desai A, Mitchison TJ. *Annu Rev Cell Dev Biol.* 1997; 13:83. [PubMed: 9442869]
19. Yu Z, Ohulchanskyy TY, An P, Prasad PN, Lin Q. manuscript submitted.
20. Yang YW, Lee JS, Kim I, Jung YJ, Kim YM. *Eur J Pharm Biopharm.* 2007; 66:260. [PubMed: 17182232] b) In our in vitro analysis, IPFA was stable in the presence of 10 mM glutathione in deuterated DMSO/PBS buffer (7:3); see Fig. S10 in ESI for details.
21. a) Matesanz R, Rodríguez-Salarichs J, Pera B, Canales A, Andreu JM, Jiménez-Barbero J, Bras W, Nogales A, Fang W-S, Díaz JF. *Biophys J.* 2011; 101:2970. b) Miller ML, Roller EE, Zhao RY, Leece BA, Ab O, Baloglu E, Goldmacher VS, Chari VJ. *J Med Chem.* 2004; 47:4802. [PubMed: 15369381]

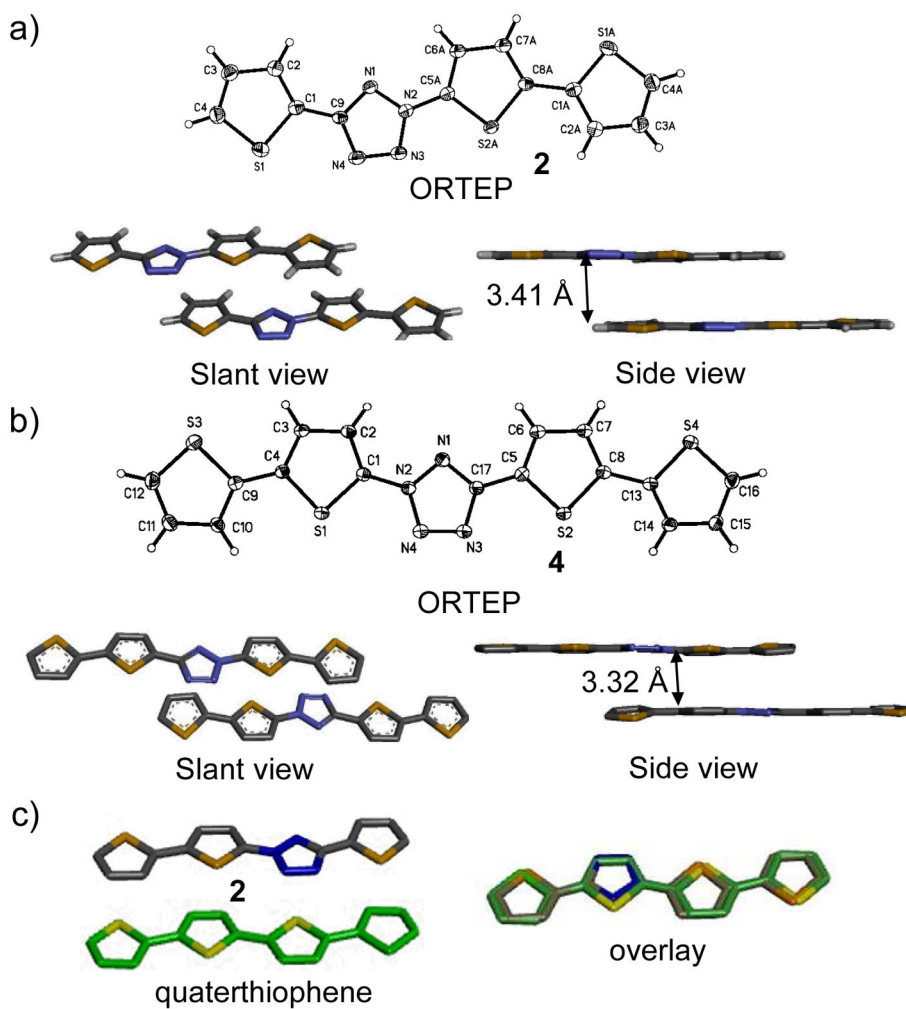


**Fig. 1.** Crystal structures of tetrazoles **2** (a) and **4** (b) and their packing in the crystals. (c) Overlay of the crystal structures of tetrazole **2** with that of quaterthiophene.

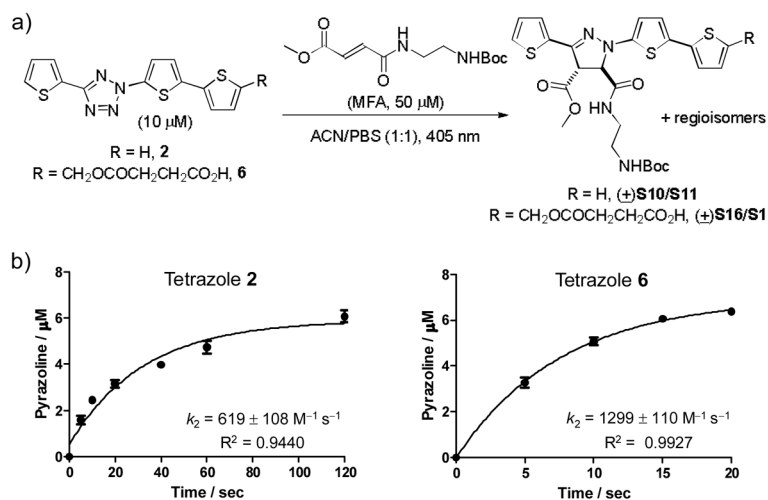


**Fig. 2.** Kinetic characterization of tetrazoles **2** and **6** in 405 nm laser-induced photoclick chemistry. (a) Reaction scheme. (b) Plots of time course of the reactions. The reactions were set up by incubating 10  $\mu\text{M}$  of tetrazole and 50  $\mu\text{M}$  of mono-methyl fumarate amide in acetonitrile/PBS (1:1), and the mixtures were illuminated with a 405-nm diode laser for the indicated time. The reaction mixtures were analyzed by reverse-phase HPLC. The amount of pyrazoline adducts was quantified by comparing the peak area to a standard curve. The photoinduced reactions were repeated three times at each time points to obtain standard deviations.



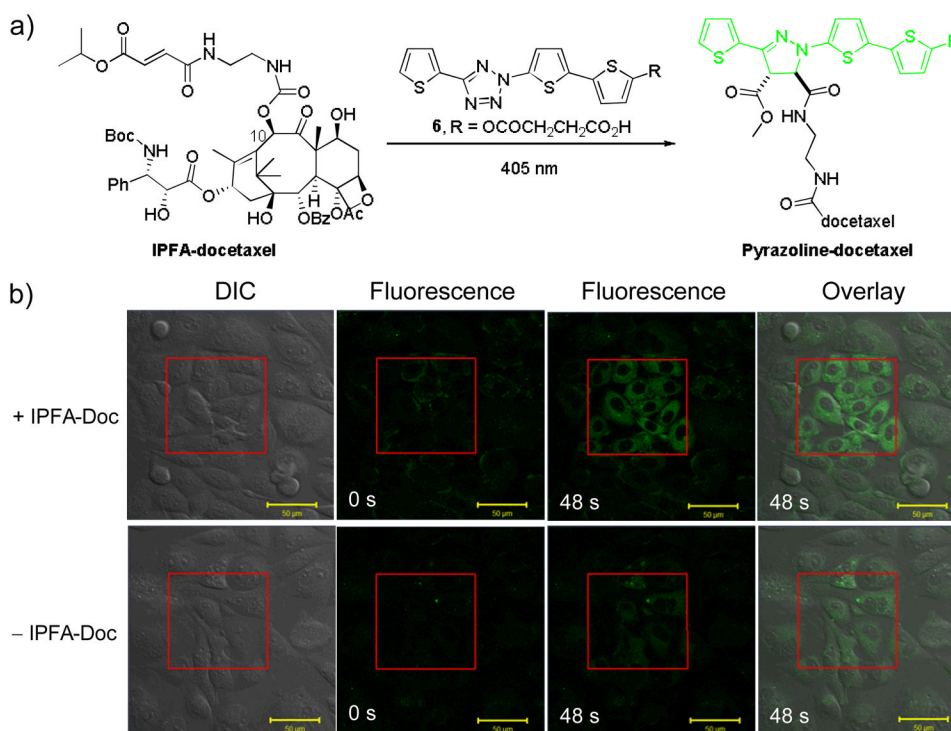
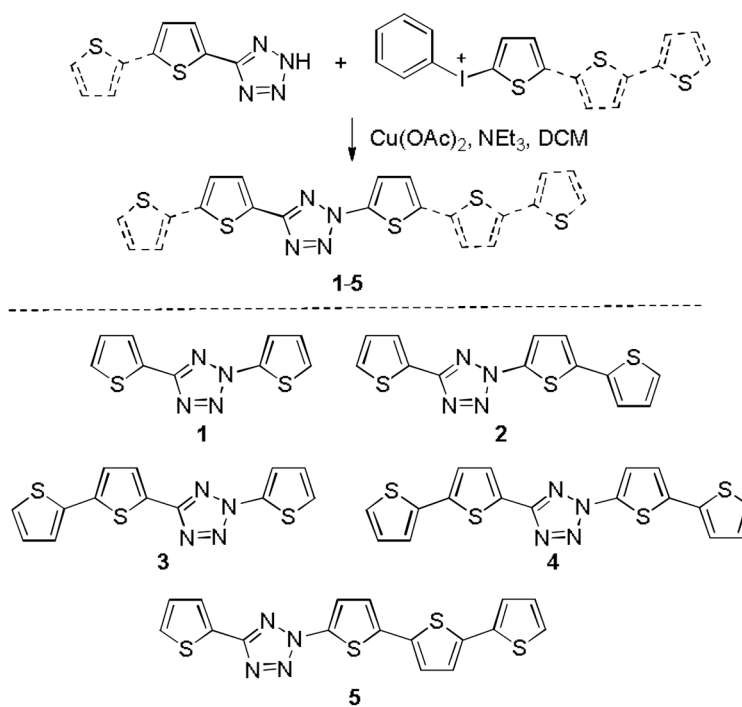


**Fig. 3.** Spatiotemporally controlled imaging of microtubules *via* laser-triggered docetaxel-directed photoclick chemistry with terthiophene-tetrazole **6**. (a) Reaction scheme. (b) Confocal micrographs of CHO cells treated with 40  $\mu$ M tetrazole **6** in the presence of (top row) or absence (bottom row) of 30  $\mu$ M IPFA-docetaxel. The cells in the quadrangle areas were exposed to 405 nm laser irradiation (0.15 mW) at 1.27  $\mu$ s/pixel illumination dwell followed by scanning entire viewing areas with 458 nm laser at 6.30  $\mu$ s/pixel illumination dwell; the scanning sequence was intermittently repeated for a duration of 125 sec. Scale bar = 50  $\mu$ m.



**Scheme 1.**  
Synthesis of oligothiophene-tetrazoles 1-5



Table 1

Absorption maxima, molar absorptivity and the calculated molecular orbital energy for oligothiophene-tetrazoles <sup>a</sup>

tetrazole	$\lambda_{\max}$ (nm)	$\epsilon_{\max}$ (M <sup>-1</sup> cm <sup>-1</sup> )	$\epsilon_{405}$ (M <sup>-1</sup> cm <sup>-1</sup> )	$E_{\text{HOMO}}$ (eV)	$E_{\text{LUMO}}$ (eV)	$\Delta E_{\text{LUMO-HOMO}}$ (eV)
<b>1</b>	308	7,900	ND <sup>b</sup>	-6.15	-1.59	4.56
<b>2</b>	354	21,000	1,500	-5.79	-1.86	3.93
<b>3</b>	346	21,000	ND <sup>b</sup>	-5.63	-1.71	3.92
<b>4</b>	366	29,000	8,300	-5.58	-1.91	3.67
<b>5</b>	390	27,000	23,000	-5.51	-2.01	3.50

<sup>a</sup> UV-Vis absorbance was measured by dissolving tetrazoles **1-5** in acetonitrile/PBS (2:1) to derive the final concentration of 15  $\mu\text{M}$ . DFT calculations were performed at the B3LYP/6-31G\* level in vacuum using SPARTAN'08 program.

<sup>b</sup> Absorption at 405 nm was not detected.